JOURNAL OF THE ROYAL SOCIETY Interface

J. R. Soc. Interface (2011) **8**, 1104–1113
doi:10.1098/rsif.2010.0594
Published online 19 January 2011

Multiplexed protein analysis using encoded antibody-conjugated microbeads

Nora Theilacker[1], Eric E. Roller[2], Kristopher D. Barbee[2], Matthias Franzreb[1] and Xiaohua Huang[2,*]

[1]*Institut für Funktionelle Grenzflächen, Karlsruhe Institute of Technology (KIT), Hermann-von-Helmholtz-Platz 1, 76344 Eggenstein-Leopoldshafen, Germany*
[2]*Department of Bioengineering, University of California, San Diego, 9500 Gilman Drive, La Jolla, CA 92093-0412, USA*

We describe a method for multiplexed analysis of proteins using fluorescently encoded microbeads. The sensitivity of our method is comparable to the sensitivity obtained by enzyme-linked immunosorbent assay while only 5 μl sample volumes are needed. Streptavidin-coated, 1 μm beads are encoded with a combination of fluorophores at different intensity levels. As a proof of concept, we demonstrate that 27 microbead populations can be readily encoded by affinity conjugation using three intensity levels for each of three different biotinylated fluorescent dyes. Four populations of encoded microbeads are further conjugated with biotinylated capture antibodies and then combined and immobilized in a microfluidic flow cell for multiplexed protein analysis. Using four uniquely encoded microbead populations, we show that a cancer biomarker and three cytokine proteins can be analysed quantitatively in the picogram per millilitre range by fluorescence microscopy in a single assay. Our method will allow for the fabrication of high density, bead-based antibody arrays for multiplexed protein analysis using integrated microfluidic devices and automated sample processing.

Keywords: multiplexed protein immunoassays; combinatorial encoding; microbeads

1. INTRODUCTION

The analysis of human serum for different biomarkers holds promise for the early detection, diagnosis and treatment of a variety of diseases, such as cystic fibrosis, arthritis and multiple types of cancer. Serum biomarkers can be used as indicators of the state of disease progression or simply as indicators for the functioning of normal biological processes within the human body. Ultimately, these biomarkers can monitor the progress of therapy [1,2]. For routine analysis of only one or a few analytes, the enzyme-linked immunosorbent assay (ELISA) remains the workhorse method for protein analysis in basic research and clinical diagnostics. Owing to increasing efforts in recent years in biomarker discovery [3,4], many high-quality antibodies with high specificity and affinity are becoming available to these markers and to entire proteomes [5–8] for basic research, early detection of cancer and other medical diagnostics [9,10].

Mass spectrometry has emerged as a powerful tool for comprehensive protein analysis in recent years [11–14]. However, no more than a few samples can be analysed at a time with this methodology. In addition, lower sensitivity for the detection of low-abundance or small proteins compared with ELISA and lengthy sample preparation accompanied with the risk of protein degradation present further challenges for the utility of this method [1].

Antibody microarray technology enables the miniaturization and parallelization of immunoassays and is now becoming a powerful tool for multiplexed protein analysis [10,15–18]. Conventionally, antibody arrays can be fabricated using a variety of robotic spotting and printing techniques for the immobilization of antibodies on a chip surface [19–22]. The typical spots for each antibody type on a conventional microarray are relatively large (2500–10 000 μm^2). These spot sizes are not suitable for protein analysis of small sample volumes such as those from single cells [19,23]. Fortunately, these issues can be resolved by conjugating antibodies to encoded microbeads that are subsequently deposited onto a surface [24–28]. The surface area occupied by each particle is three to four orders of magnitude smaller (approx. 1 μm^2) than the typical antibody spot size, thus allowing for higher multiplexing on arrays with much smaller footprints. In addition, the antibody-conjugated microbeads can be stored in a buffer

*Author for correspondence (x2huang@ucsd.edu).

Received 26 October 2010
Accepted 15 December 2010

solution prior to assembly of the microfluidic device, thereby reducing the risk of denaturation of the immobilized antibodies. Antibodies capable of detecting a wide range of antigens can be coupled individually to encoded microbeads prior to use and the combination of these antibody-conjugated microbeads can be customized depending on the target proteins. Antibody-conjugated microbeads can also be used in the so-called 'suspension bead array' platform such as the Luminex system where assays are performed in suspension in microwell filter plates, and flow cytometry is used to decode the microbeads and quantify the fluorescence signal [29–31].

There are many commercially available microbeads with a wide range of surface chemistries suitable for antibody conjugation and they can be encoded by a variety of techniques [32]. A large number of microbeads can be encoded using various combinations of fluorescent dyes or quantum dots with different emission wavelengths and intensity levels usually by entrapping the fluorescent moieties in the interior of the microbeads [33–36], or by covalently attaching the dyes onto the surface of the microbeads [33,37]. Up to 500 distinct 5.6 μm microbeads that are encoded using three colours and different levels of intensity are available from Luminex Corporation. By combining the bead-based immunoassays with a dedicated flow cytometer for signal detection and instruments for automated fluidic handling, very high-throughput multiplexed protein analysis is now feasible [31,38].

In this study, we describe the proof of concept of a method for rapid encoding of 1 μm beads for multiplexed protein analysis using an integrated microfluidic device. Here, smaller microbeads are more desirable for the assembly of very high-density arrays and efficient epifluorescence imaging with high numerical aperture objectives [23,39–41]. Instead of the internal encoding strategy, which involves swelling of the microbeads with organic solvents and the entrapment of fluorescence moieties, we use an external encoding strategy, similar to the one reported by Fergusson *et al.* [33]. We make use of commercially available 1 μm superparamagnetic microbeads that have been pre-functionalized with streptavidin on the surface for rapid encoding and conjugation of antibodies. Various combinations of fluorescent dyes with well-separated excitation and emission spectra and intensity levels thereof are used to encode the beads. Once encoded, the microbeads are conjugated with biotinylated antibodies and then assembled onto a glass surface. We immobilize the microbeads on derivatized glass coverslips using a permanent magnet and a carbodiimide coupling chemistry. The immobilization and all downstream processes are performed within a flow cell that is formed between the glass coverslip and a silicon dioxide-coated aluminium plate using a pre-cut gasket. The custom-built aluminium plate has tapped ports that allow for tubing connections. Samples and reagents are introduced into the channel using a computer-controlled syringe pump. This design allows for automated, high throughput and multiplexed protein analysis. Figure 1 illustrates the protein assay procedure (figure 1*a*) and an exploded view of the device (figure 1*b*).

2. METHODS

2.1. Microbead encoding

Streptavidin-coated polystyrene microbeads (Dynabeads MyOne Streptavidin C1, Cat. no. 650-01, Invitrogen Corp.) were encoded with three different biotinylated fluorophores (Alexa Fluor 488 biocytin, Cat. no. A-12 924, Alexa Fluor 594 biocytin, Cat. no. A-12922, Invitrogen Corp., and Atto 680-Biotin, Cat. no. 55819, Sigma-Aldrich Corp.). More specifically, 10, 30, and 100 pmol of each fluorophore were used per microgram of microbeads to encode the three intensity levels of each dye. The combinations of fluorescent dyes and intensity levels were chosen such that 27 different microbead populations could be uniquely identified. Three different amounts of Alexa Fluor 488 were diluted in PBST (phosphate-buffered saline (PBS) plus Tween 20: 137 mM sodium chloride, 2.7 mM potassium chloride, 10 mM sodium phosphate dibasic, 2 mM potassium phosphate monobasic, 0.05% Tween 20, pH 7.4) to give a final volume of 600 μl. Coupling was performed by adding each fluorophore solution to a microbead suspension (30 μg in 150 μl PBST). After the addition of each aliquot, the suspensions were vortexed to mix the dyes thoroughly with the microbeads. Next, three Alexa Fluor 594 solutions were prepared as described above. Each solution was divided into three aliquots and subsequently added to one third of each microbead suspension, yielding nine different encoded microbead suspensions of 10 μg each. The third fluorophore was conjugated to the beads in a similar way. Each bead suspension was again divided into three aliquots and three different amounts of Atto 680 fluorophore were added to the aliquots. Following the addition of the last aliquot, the microbeads were incubated under rotation for 15 min at a final microbead concentration of 20 $\mu g\,ml^{-1}$. The microbeads were separated magnetically, washed twice with PBST and stored at 4°C.

2.2. Biotinylation of antibodies and conjugation of antibodies to encoded microbeads

Four different antigens together with matching antibody pairs were used as a model system for multiplexed protein detection. These included a monoclonal antibody (anti-PSA, Cat. no. 304-01, Fujirebio Diagnostics, Inc.) against human prostate-specific antigen (PSA, Cat. no. 1344SE, R&D Systems, Inc.), monoclonal antibodies (Cat. nos. MAB206 and MAB208, R&D Systems) against human interleukin-6 and human interleukin-8 (IL-6, Cat. no. 206-IL and IL-8, Cat. no. 208-IL, R&D Systems), and a monoclonal antibody against human tumour necrosis factor-α (anti-TNF-α, Cat. no. 13-7349 and TNF-α, Cat. no. 14-8329, eBioscience, Inc.). The monoclonal antibody against TNF-α was biotinylated by the supplier. Prior to using this protein combination for multiplexing, we performed our assays using two

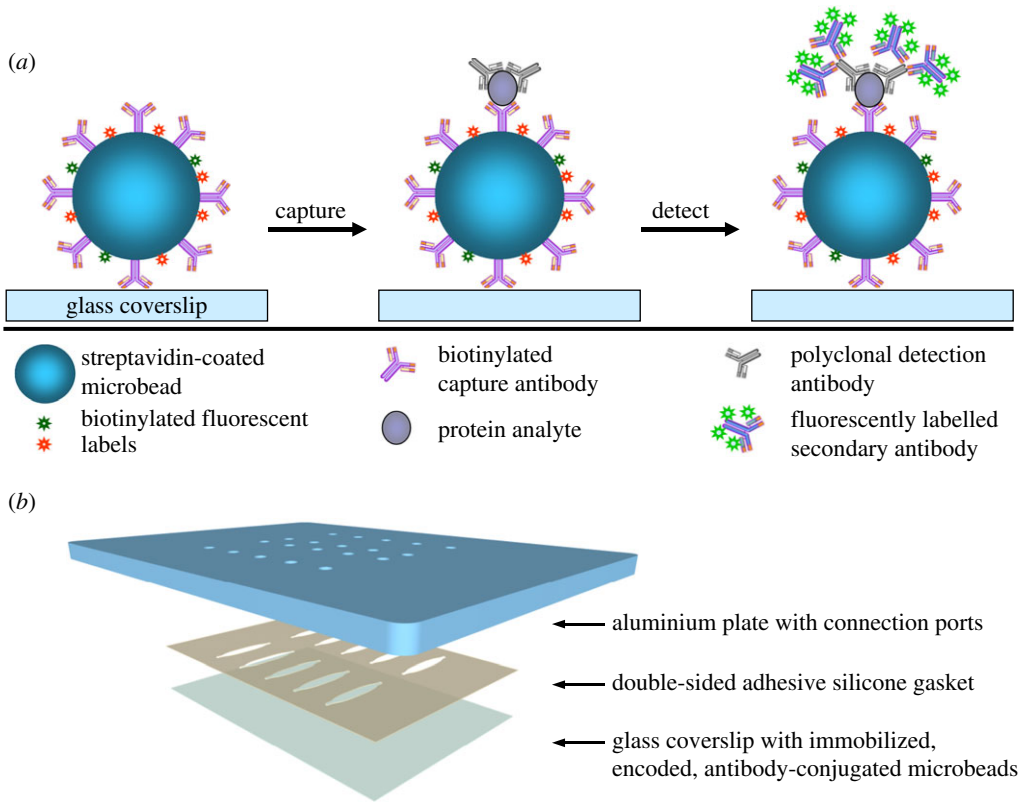

Figure 1. Assay strategy and fluidic device for protein analysis with antibody-conjugated, encoded microbeads. (*a*) Strategy and procedure. Biotinylated capture antibody is conjugated to the encoded microbead and covalently coupled to the glass surface. Then the protein solution is introduced into the flow cell. After the protein analyte has been captured, a polyclonal detection antibody is added to the sample. A fluorescently labelled secondary antibody specific to the polyclonal detection antibody is used to quantify the protein analyte by fluorescence imaging. (*b*) Fluidic device. Shown is an exploded view of the device with 10 channels consisting of an aluminium plate (top) with ports for fluidic connectors, a double-sided adhesive silicone gasket with 10 channel cutouts (middle) and a derivatized glass coverslip (bottom).

cancer markers, human epidermal growth factor receptor 2 (ErbB2) and cysteine-rich secretory protein 3 (CRISP3), and their corresponding monoclonal antibodies (Cat. no. 2397-CR and MAB2397 for CRISP3 and Cat. no. 1129-ER and MAB1129 for ErbB2, R&D Systems) instead of IL-6 and IL-8. Unconjugated monoclonal antibodies were covalently labelled with *N*-hydroxysuccinimide (NHS) ester-activated biotin molecules via a long polyethylene glycol (PEG) linker. The antibodies were biotinylated by mixing 1.35 µl of a 4.95 mM NHS–PEG_{12}–biotin solution (Cat. no. 21312, Pierce Biotechnology, Inc.) in dry *N*,*N*-dimethylformamide with 50 µl of a 1 mg ml^{-1} antibody solution in PBS. The mixture was allowed to react at room temperature for 30 min. Unconjugated biotin molecules were then removed using spin columns as described by the manufacturer (Cat. no. 89882, Pierce Biotechnology, Inc.).

Biotinylated monoclonal antibodies were conjugated to encoded microbeads by adding the microbead suspension (20 µg microbeads in 380 µl PBST) to the antibody solution (4 µg antibody in 20 µl PBST) stepwise in ten 38 µl aliquots to prevent the aggregation of the beads. After the addition of each aliquot, the suspension was vortexed to mix the antibodies thoroughly with the microbeads. Following the addition of the last aliquot, the microbeads were incubated under rotation for 30 min at room temperature, separated magnetically, washed four times with PBST and then stored at 4°C.

2.3. Activation of glass coverslips and immobilization of encoded microbeads

The flow cell used for immobilization and subsequent imaging of the encoded microbeads consisted of a carboxylated glass coverslip, a thin double-coated adhesive silicone gasket with 12 cutouts for the flow channels, and an aluminium plate with ports for tubing connection to a syringe pump (Cavro XR Rocket Pump, Tecan Group, Ltd). To prepare the carboxylated substrates, 50 × 75 × 0.170 mm borosilicate glass coverslips (Erie Scientific) were washed in batch mode with a 2 per cent Micro-90 detergent solution (Cole-Parmer) and rinsed with 18 MΩ cm deionized water (dH_2O). They were then cleaned by soaking in acetone and then in methanol for 30 min each in an ultrasonic bath and rinsed once with dH_2O. Next, the coverslips were cleaned in a 1 : 4 mixture of 68 per cent HNO_3 : dH_2O for 60 min followed by washes with dH_2O and then dipped in methanol for 1 min. After the coverslips were dried at 110°C for 15 min in a gravity convection oven and cooled to room temperature, they were placed in a 2 per cent solution of 3-aminopropyltriethoxysilane (Gelest Inc.) in 95 : 5 ethanol : dH_2O at room temperature for 5 min, rinsed three times with

acetone and cured at 110°C for 10 min in a gravity convection oven. The coverslips were then treated with a 250 mM solution of succinic anhydride (Thermo Fisher Scientific Inc.) in dry *N*,*N*-dimethylformamide with 250 mM triethylamine. After a 2 h incubation at room temperature, the coverslips were rinsed three times with acetone and once with methanol and then dried in a vacuum desiccator.

Prior to use, one coverslip was attached to the custom-built aluminium plate using a double-sided silicone tape (no. 702, Scapa Group) with pre-cut channels (figure 1*b*). The channels were designed with a computer-aided design program and cut out of the approximately 100 μm thick tape using a cutting plotter (CC200-20, Graphtec Corp.). Each channel was 15 mm long and 5 mm wide with 1 mm diameter inlet and outlet ports creating a total volume of about 5 μl. The aluminium plate contained 24 threaded boss ports for connecting each flow channel to a syringe pump via 062 MINSTAC fittings (The Lee Co.). To immobilize the encoded microbeads covalently, each channel was incubated for 20 min with 50 mM 2-(*N*-morpholino)ethanesulphonic acid (MES) buffer at pH 5 containing 100 mM 1-ethyl-3-(3-dimethylaminopropyl)carbodiimide (EDC) and 10 mM sulpho-NHS and then washed with 50 mM MES buffer. A 10 μl aliquot of the antibody-conjugated microbead suspension (50 μg ml^{-1} in PBST) was introduced into each channel and a permanent magnet was briefly dragged along the back side of the coverslip to direct the rapid coupling of the microbeads onto the activated surface. Unbound microbeads were washed away with PBST.

2.4. Multiplexed immunoassays

Four encoded, antibody-conjugated microbead populations (50 μg ml^{-1}) were pooled and then immobilized onto the channel surface as described above. Stock antigen solutions were diluted in PBS with 1 per cent bovine serum albumin (BSA) or directly in foetal bovine serum to the desired concentrations. One per cent BSA in PBS or foetal bovine serum served as controls for non-specific binding and background subtraction. After the beads were blocked using a solution of 1 per cent BSA, 5 per cent sucrose, 0.01 per cent NaN_3 in PBS, pH 7.4 for 20 min and washed with 50 μl PBST, a 10 μl aliquot of the antigen sample or control was introduced into each channel. The antigens were allowed to bind to the microbeads at room temperature for 90 min. The channels were then washed with PBST. Polyclonal detection antibodies (Cat. nos. AF206, AF208, AF1344, R&D Systems and Cat. no. ab9635, Abcam Inc.) were diluted to 1 μg ml^{-1} each in PBS with 1 per cent BSA and introduced into the channels. After a 60 min incubation, the channels were washed again with PBST and a 10 μl aliquot of secondary antibodies labelled with Alexa Fluor 680 (Cat. no. A21 084 and Cat. no. A10 043, Invitrogen Corp.) diluted to 2 μg ml^{-1} in 1 per cent BSA in PBS was introduced into each channel. After a 30 min incubation at room temperature, the channels were washed with PBST and quantitative fluorescence imaging was performed.

2.5. Enzyme-linked immunosorbent assay

ELISAs were performed to compare the sensitivity of our multiplexed system with that of a conventional sandwich immunoassay. Monoclonal capture antibodies were diluted in PBS (2 μg ml^{-1}) and added to the wells of a microtitre plate. The plate was then incubated overnight at 4°C. Each well was washed five times with PBST and blocked for 60 min with the same blocking solution used in the microbead assay. Stock antigen solutions were diluted in PBS with 1 per cent BSA or in foetal bovine serum to the desired concentrations. One per cent BSA in PBS or foetal bovine serum served as controls. The plate was washed again and 100 μl of the samples were added into each well. The antigens and control sample were allowed to bind at room temperature for 90 min. After another washing step, the polyclonal detection antibody (1 μg ml^{-1} in PBS with 1 per cent BSA) was added into the wells and incubated for 60 min. The plate was washed again with PBST and secondary horseradish peroxidase conjugated antibody (Cat. no. 25-787-278475 or Cat. no. 25-787-278487, Genway Inc.) was added. After a 60 min incubation at room temperature, the plate was washed with PBST and 100 μl of tetramethylbenzidine solution was added to each well. To stop the enzymatic reaction, 50 μl of a 1 M H_2SO_4 solution was added and the absorption of the product was measured at a wavelength of 450 nm using a plate reader.

2.6. Fluorescence imaging and microbead decoding

Fluorescence imaging of the encoded microbeads was performed on an epifluorescence microscope (Axio-Observer.Z1, Carl Zeiss, Inc.) with a 20×/0.8 NA dry objective. The excitation light was provided by an instrument with a 300 W xenon arc lamp and high-speed wavelength-switching capability (Lambda DG-5, Sutter Instrument Co.) in combination with filter cubes matching the three different excitation and emission wavelengths of the fluorophores (FITC-3540B for Alexa 488, TXRED-4040B for Alexa 594, Cy5.5-A for Alexa 680 and Atto 680, Semrock Inc.). The microscope was also equipped with a motorized stage with linear encoders (BioPrecision 2, Ludl Electronics Products, Ltd) and an EMCCD camera with 1004 × 1002 pixels with a pixel size of 8 × 8 μm for ultra-sensitive fluorescence imaging (iXon+ 885, Andor Technology, PLC). Precise focusing was achieved and maintained using an autofocusing system (Definite Focus System, Carl Zeiss, Inc.), which uses an 835 nm light-emitting diode to reflect light off the surface of the coverslip for focus feedback. For each field of view, images were taken using the appropriate filter cubes in all three fluorescence channels. Quantitative fluorescence imaging was fully automated with custom software.

Image analysis was automated using a custom macro written for ImageJ, a Java-based software program [42]. First, the images of both encoding channels were merged. Then a mask was created by applying the Otsu thresholding filter to the image [43]. This mask was later used to identify the positions of the

microbeads in each field of view. Microbead doublets, aggregates or other artefacts were located by particle size analysis and removed from the mask. Microbeads with a significantly lower intensity could not be identified by applying the Otsu thresholding filter. Therefore, another mask that included microbeads with high fluorescence intensity and aggregates was created and the pixel-values of this mask were set to zero. The original image was then multiplied with the zero-mask. This operation removed microbeads with high fluorescence intensity levels and aggregates from the image, and allowed for the identification of microbeads with low fluorescence intensity. The masks of high- and low-fluorescence intensity microbeads were subsequently merged and used to obtain the fluorescence intensities of each single bead in all three channels. Further data processing was performed using Matlab (The MathWorks, Inc.).

3. RESULTS AND DISCUSSION

3.1. Combinatorial microbead encoding

To demonstrate our strategy for microbead encoding and subsequent protein detection, four microbead populations were encoded with a combination of the two fluorophores Alexa Fluor 488 and Alexa Fluor 594 at two intensity levels. The intensities of the four bead populations in both fluorescent channels are shown in figure 2*a*. Each colour represents one population of approximately 1000 beads with one dot representing one microbead. These distinctive combinations of fluorophores can be used to encode a unique antibody-conjugated microbead population for future use in the pool of antigen-capturing microbeads for multiplexed protein assays. In such assays, only one type of capture antibody is conjugated to a given encoded microbead population. We conjugated IL-8 capture antibodies to the bead population labelled no. 1 in figure 2*a*, and TNF-α, PSA and IL-6 capture antibodies to populations nos. 2–4, respectively.

To demonstrate the ability for higher multiplexing, we used a combination of three fluorophores, Alexa Fluor 488, Alexa Fluor 594 and Atto 680, at three intensity levels (approx. 6000, 20 000 and 60 000 fluorophore molecules per microbead) to encode 27 different bead populations. The fluorophores occupied between 1.2 and 12 per cent of the biotin-binding sites on each microbead, leaving sufficient binding sites for conjugation of biotinylated antibodies on the microbead surface. According to the manufacturer, one single microbead can bind up to 1.5 million free biotin molecules, but only about 90 000 antibody molecules. A maximum of 12 per cent (180 000, 60 000 molecules each of all three different dyes) of the binding sites are occupied by the biotinylated dye molecules used for encoding. Hence, theoretically 1.32 million binding sites for free biotin molecules are still available on the microbead surface and this amount is probably enough to bind the maximum number of antibodies (90 000), even after the microbeads have been encoded with biotinylated fluorophores. The fluorescence intensities of the three dyes encoding the 27 microbead populations are illustrated in three dimensions in figure 2*b*. Each axis represents one fluorescent channel and each colour represents one population of approximately 250 encoded beads. For clarity in visualization, the data are presented with two selected axes in figure 2*c*,*d*. It is apparent that the clusters, each representing different bead populations, are well separated and can be distinguished easily.

Theoretically, the maximum number of distinctly encoded microbead populations is determined by the number of fluorescent dyes with distinguishable emission wavelengths (m) and fluorescence intensity levels (n), with the total number of unique combinations being n^m. The number of encodings that can be practically created depends on the potential variations in the fluorescence intensity, and our ability to quantitatively measure the intensity levels of the fluorophores with different emission characteristics. As indicated by the scattered intensities of each bead population in figure 2, there is a slight variation in the fluorescence intensity among the beads of the same population. Ideally, each population of uniquely encoded microbeads should occupy only a very tight spot in intensities if all microbeads had exactly the same size, number of biotin-binding sites and equal number of bound fluorophores. The observed variation in intensity could be due to several factors, including the non-uniformity of the microbeads in terms of bead size and number of biotin-binding sites on each microbead, and the stochastic variation in fluorophore binding to the microbeads during the encoding process. We found that the variation in the encoding procedure can be reduced by adding a relatively large volume of fluorophores stepwise to a small volume of microbeads. Such a procedure allows for even distribution of the fluorophore molecules among the microbeads.

Additional variation in intensity levels is due to a slight non-uniformity in excitation and other optical effects across the field of view in fluorescence imaging. Image processing may also introduce some variation. For example, the images of different fluorescent channels from the same field of view are aligned prior to analysis. This alignment only allows for shifts in increments of full pixels. If the actual image is shifted a fraction of a pixel, the correct bead position is compromised, resulting in deviations in intensity measurements. To minimize this potential deviation, we use a slightly larger number of pixels for each bead to ensure that the intensity of each bead is fully accounted for. However, depending on the variation of the residual background intensity of the image following background subtraction, the background pixels included in the analysis region of a particular bead can contribute noise to the calculated intensity. This limitation could potentially be alleviated by using an additional fluorescent dye as a standard to normalize the intensities of the other fluorophores. The distribution of fluorescence intensity of each microbead population as observed in figure 2 is still relatively tight. As more populations are added, the clusters will get closer and eventually overlap, making decoding difficult or impossible. It is, however, clear that more than 27 microbead populations could be encoded and decoded. With our imaging system, six organic fluorophores with

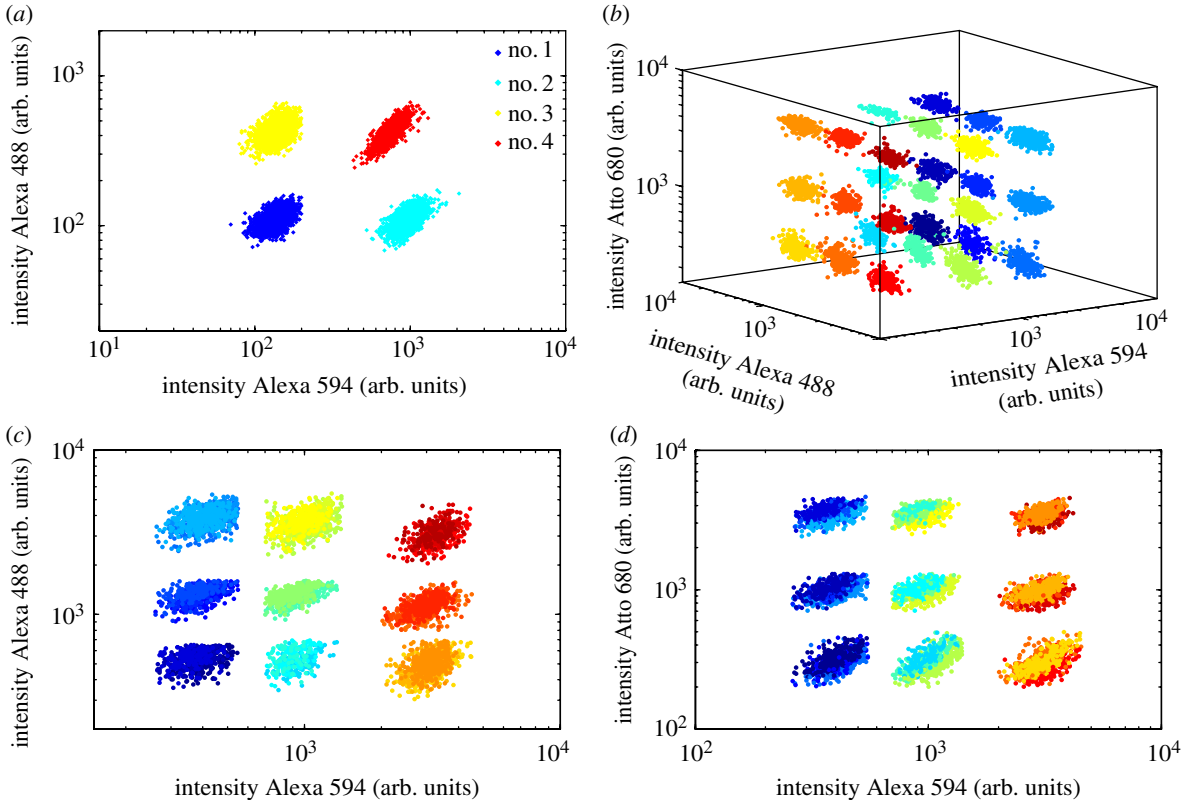

Figure 2. Encoding of microbeads using a combination of different fluorophores at various intensity levels. The mean intensity of each bead in one fluorescence channel is plotted against the second fluorescence channel (coloured dots). Each colour represents one microbead population. (*a*) Encoding of four microbead populations using two fluorophores at two intensity levels. (*b*) Twenty-seven microbead populations encoded with three fluorophores at three intensity levels. Fluorescence intensities in the Alexa Fluor 594, Alexa Fluor 488 and Atto 680 channels are plotted on the *x*, *y* and *z*-axes, respectively. Owing to variation in the fluorescence intensity in each encoded microbead population, some dots scatter in between the clusters. Those dots (approx. 10% of the total) are excluded and not shown in the plot. (*c*,*d*) The intensities of the encoded microbeads as shown in (*b*) are plotted as two-dimensional graphs, with the intensities in the Alexa Fluor 488 channel (*c*) and Atto 680 channel (*d*) plotted against the intensity of the Alexa Fluor 594 channel.

different fluorescence wavelengths can be spectrally resolved. If one colour is reserved for protein detection, the other five colours can be used for encoding. This means that using only three intensity levels of fluorophores, 243 ($=3^5$) distinct encodings could be generated with our current instrument. Further work will be required to demonstrate the full encoding capability.

3.2. *Multiplexed protein immunoassays and sensitivity*

To demonstrate the utility and sensitivity of our method for protein analysis, we used four different encoded and antibody-conjugated microbead populations to perform immunoassays of four proteins. These include IL-6, IL-8 and TNF-α, which are used as biomarkers to monitor a variety of diseases, and PSA, a marker for prostate cancer. As shown by the standard curves in figure 3, we demonstrated the feasibility of quantifying four antigens in multiplexed protein assays. We used a mixture of the four encoded microbead populations shown in figure 2*a*, each conjugated to a specific capture antibody to assay the four proteins individually while simultaneously monitoring the background signal of the three other microbead populations. All assays were performed in both 1 per cent BSA and serum. The fluorescence signal obtained from microbeads incubated with the control sample (no antigen) was used to standardize the signal. More specifically, the fluorescence signal of the control was set to one, and the relative fluorescence intensity (the *y*-axis value in figure 3*a*–*c*) was calculated as the ratio between the mean fluorescence signal of microbeads incubated with antigen and the control without antigen. We also obtained standard curves for the antigens spiked into 1 per cent BSA and serum using ELISA. Table 1 summarizes the limit of detection (LOD) and coefficient of variation (CV) of the multiplexed bead assays and ELISAs. The LOD was calculated by adding two standard deviations to the measured value of the control. All R^2 values obtained by the 5 parameter logistic fit (5-PL fit) [44] are greater than 0.99. The LOD in our bead assay can be as low as 1 pg ml^{-1} for IL-8 in 1 per cent BSA in comparison with a LOD of 5 pg ml^{-1} for ELISA. For IL-6 and PSA, the detection limits of the bead assays are similar or slightly higher than those obtained by ELISA.

The LOD for TNF-α in the multiplex bead assay is two to three orders of magnitude higher in comparison with ELISA. We also observed that microbeads coupled with TNF-α capture antibody displayed a high overall fluorescence signal as shown in figure 3*d*. To investigate

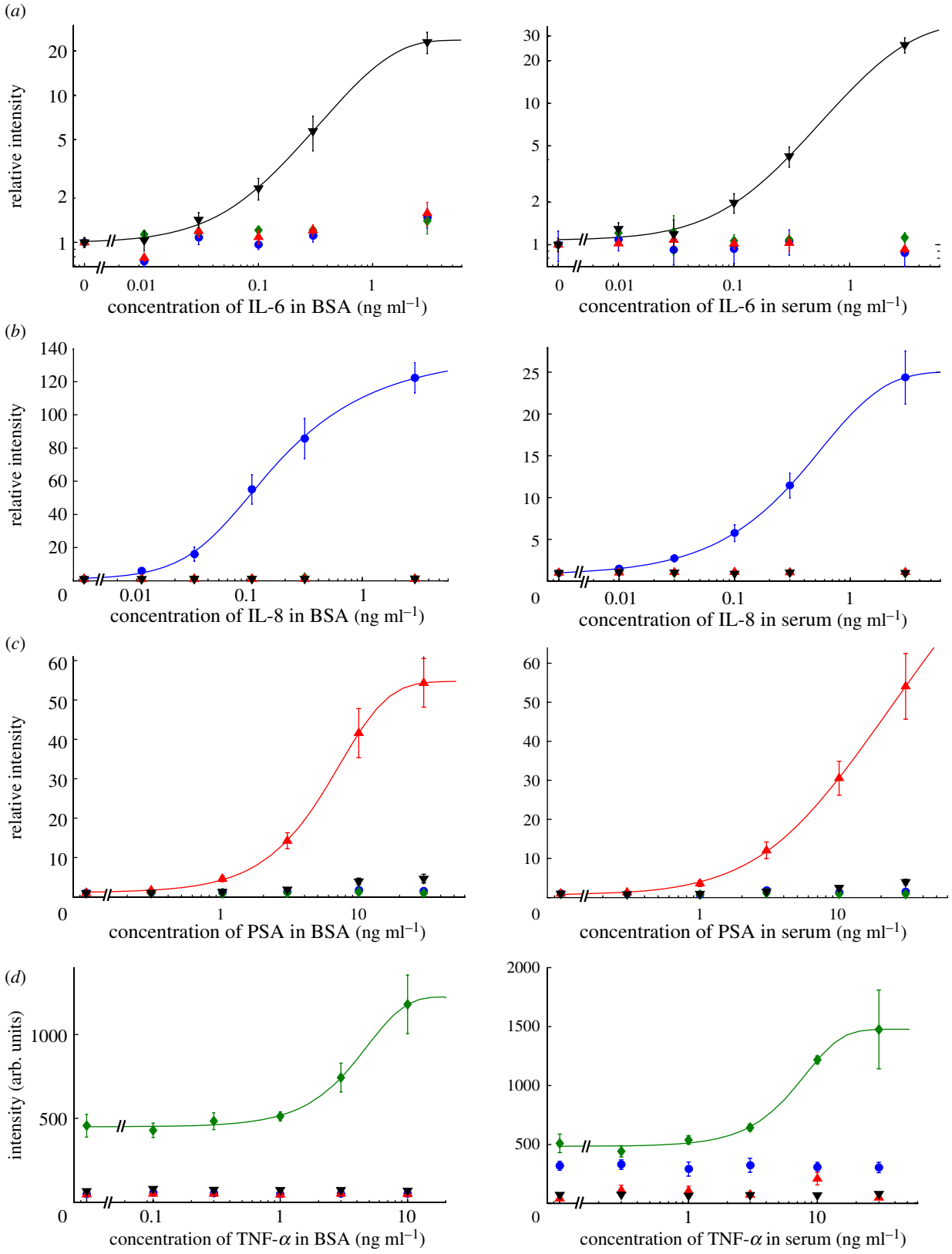

Figure 3. Multiplexed immunoassay performance. Sensitivity assays were performed using the proteins (*a*) IL-6, (*b*) IL-8, (*c*) PSA and (*d*)TNF-α, diluted in PBS with 1% BSA or in foetal bovine serum. The data in (*a*–*c*) are standardized. In (*d*), the raw data without background subtraction are shown to indicate the high background fluorescence owing to non-specific binding of IL-6 and IL-8 detection antibodies to the TNF-α capture antibody. (*a*–*d*) Solid lines, 5PL fit; blue circles, IL-8; green diamonds, TNF-α; red triangles, PSA; inverted black triangles, IL-6.

this large discrepancy, we performed an ELISA using TNF-α capture antibody to coat the wells, different dilutions of TNF-α in 1 per cent BSA and the detection antibodies against IL-6 and IL-8 in combination with their respective secondary antibodies. As indicated in figure 4*a*, we observed that both the detection

Table 1. Comparison of protein detection limits using ELISA and multiplexed encoded microbeads.

	ELISA (pg ml^{-1})		multiplexed bead assay (pg ml^{-1})	
antigen	in 1% BSA (CV)[a]	in serum (CV)	in 1% BSA (CV)	in serum (CV)
IL-6	4.3 (4.0%)	2.2 (3.0%)	16.7 (10.9%)	22.3 (14.0%)
IL-8	4.5 (5.9%)	15.0 (6.6%)	1.1 (11.3%)	7.8 (12.3%)
PSA	15.8 (5.7%)	36.3 (2.7%)	81.1 (13.7%)	212.3 (16.2%)
TNF-α	26.3 (7.4%)	13.0 (2.7%)	1700 (9.9%)	3210 (17.3%)
			273.8[b] (16.3%)	371.2[b] (15.4%)

[a]Coefficient of variation (CV), which is the ratio of the standard deviation to the mean value. In the table, the mean of all CVs of one experiment is given. For ELISA, the CV corresponds to the mean of eight CVs from the measurements of eight different antigen concentrations. For the microbead assay, the CV corresponds to the mean of 24 CVs for each bead experiment (four bead populations at six different antigen concentrations).
[b]Assays were performed in the presence of all four encoded microbead populations, with one bead type conjugated to a specific monoclonal antibody against CRISP3, ErbB2, PSA and TNF-α, respectively.

antibodies for IL-6 and IL-8 bind non-specifically to the capture antibody against TNF-α. We noticed that there is also some non-specific binding of serum proteins to the microbeads conjugated with IL-8 capture antibody, which is not observed when the assay is performed in the presence of 1 per cent BSA (figure 3*d*). We had performed other multiplexed protein assays prior to using the current combination of antigens and capture microspheres. We were able to detect TNF-α at concentrations of 270 and 370 pg ml^{-1} in 1 per cent BSA and serum, respectively, in the presence of three other bead populations with capture antibodies against ErbB2, PSA and CRISP3, all of which did not show a significant background (figure 4*b*,*c*). Therefore, it is feasible to detect TNF-α in a multiplexed protein assay using a compatible combination of capture and detection antibodies.

The detection limit of each protein depends on the quality of the antibody pairs as well as the assay conditions, in particular, the concentration of detection antibodies, and incubation times and temperatures. Even though we do not use enzymatic signal amplification and our sample volume is much smaller than that of the ELISA (5 µl per channel versus 100 µl per well), we are able to detect protein analytes in a concentration range similar to ELISA using fluorescently labelled antibodies and a highly sensitive EMCCD camera. The ultimate sensitivity is likely to be limited by the quality of the antibodies used and the background fluorescence from non-specific binding of analytes and antibodies to the surface of the microbeads. Higher sensitivity may be possible through further optimization of the assay conditions and the use of an objective with a higher numerical aperture. The greatest limitation of

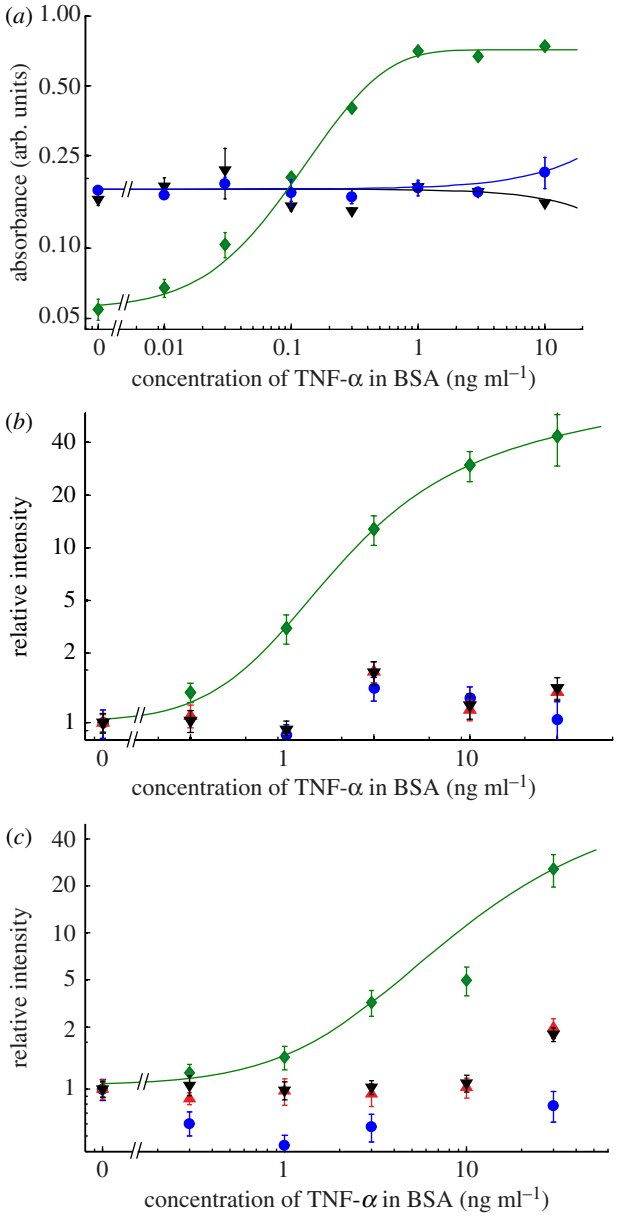

Figure 4. Cross-reactivity and detection of TNF-α in a multiplexed protein assay using a compatible combination of capture and detection antibodies. (*a*) Assessment of the non-specific binding of IL-6 and IL-8 detection antibody to TNF-α capture antibody by ELISA. (*b*,*c*) Multiplexed immunoassay performance using the proteins CRISP3, PSA, ErbB2 and TNF-α, diluted (*b*) in PBS with 1% BSA or (*c*) in foetal bovine serum. (*a*) Filled diamonds, pAb TNF-α; filled circles, pAb IL-8; inverted black triangles, pAb IL-6. (*b*,*c*) Solid lines, 5PL fit; filled circles, CRISP3; filled diamonds, TNF-α; filled triangles, PSA; inverted black triangles, ErbB2.

our methodology, like that of many multiplexed protein immunoassays, is the availability of highly specific antibody pairs with minimal or no cross-reactivity. In our multiplexed assays, we use a total of 10 different antibodies (four capture antibodies, four detection antibodies and two different fluorescently labelled secondary antibodies) to interrogate four antigens spiked into serum and BSA. The reliable and high-sensitivity multiplexed protein detection is highly dependant on the quality of all the reagents, in particular, the antibodies.

Compared with other methods for immunoassays using optically encoded microbeads [23,27], our method has several advantages. First, our encoding strategy is scalable and very easy to implement with readily available high-quality microbeads. Once the microbeads are encoded, any type of biotinylated antibody can be conjugated to them. A customized combination of encoded, antibody-conjugated microbeads can be mixed together and assembled on demand into arrays or deposited on derivatized glass coverslips within seconds [24]. Second, our assay format can be integrated into microfluidic systems for automated sample processing and analysis. Third, our flow cell is compatible with multiplexed sample processing and ultra-sensitive fluorescence imaging using an EMCCD camera and an objective with a high numerical aperture (e.g. with a 40 ×/oil NA 1.3 or 20 ×/water NA 1.0 objective). The typical sample and antibody solution volumes required for a standard ELISA range between 100 and 200 µl per well. Triplicate measurements of four proteins with ELISA would require 1–2 ml of reagents including capture, detection and secondary antibody. Only 5 µl of reagents is needed for each flow channel in our system. Therefore, only 15 µl of reagents is needed for assaying many proteins since a very large number of antibody-conjugated encoded microbeads can be accommodated in each flow channel. This significantly reduces the cost of antibodies and other reagents while allowing for the simultaneous interrogation of many proteins.

Recently, we have demonstrated that millions of DNA- or protein-conjugated microbeads can be rapidly assembled into high-density arrays on microfabricated substrates [24,25]. We have also shown that microbeads encoded internally with fluorescent dyes can be combined with a spatial encoding strategy to enable even greater multiplexing capability [26]. In this study, we show that at least 27 unique populations of microbeads can be encoded externally on the surface of the beads using three different fluorescent dyes at three distinct intensity levels. More significantly, we have demonstrated the ability for sensitive detection of four antigens spiked into serum using antibodies conjugated to the microbeads in a microfluidic device. If 1 µm beads encoded and conjugated with unique antibodies are assembled into an array with a pitch of 2 µm, as many as 2500 microbeads can be placed in a 100 × 100 µm area. If 10 encoded microbeads are used to interrogate a protein species of interest to provide 10-fold oversampling, 250 different protein species can be analysed within this 100 × 100 µm area, the typical size of one spot used in conventional printed microarrays [16,45]. Therefore, our method will enable the integration of antibody array fabrication into microfluidic devices for sensitive multiplexed protein analysis [23,39,41,46] and potentially for single cell analysis.

4. CONCLUSIONS

We have developed a method to encode 1 µm beads by using a combination of fluorophores and intensity levels. Readily available streptavidin-coated microbeads were externally encoded using biotinylated fluorophores and the encoded microbeads were further conjugated with biotinylated antibodies. As a proof of concept, we have demonstrated the ability to encode and decode 27 populations of microbeads using three fluorescence colours at three intensity levels each. We have also developed a microfluidic device for capturing the encoded, antibody-conjugated microbeads and for protein analysis. Our device and assay format are compatible with automated sample processing and ultra-sensitive fluorescence imaging. Using four populations of encoded microbeads with each population conjugated with an antibody against a specific protein, we have demonstrated that four proteins can be detected simultaneously and quantitatively via automated fluorescence imaging. Our detection limit is in the picogram per millilitre range for IL-6, IL-8 and PSA and in the low nanogram per millilitre range for TNF-α. Compared with conventional printed microarrays and ELISA, our method enables a much higher degree of miniaturization for immunoassays. Our method and device will enable highly multiplexed protein analysis with a single miniaturized device with a throughput equivalent to hundreds of immunoassays in an area as small as 100 × 100 µm. This small footprint will be particularly useful for sensitive multiplexed detection of proteins from very small volumes and single cell lysates using integrated microfabricated devices.

This work was supported in part by the National Institutes of Health (R01HG004804) and the National Science Foundation (BES-0547193, a CAREER Award to X.H.). N.T. was supported by Karlsruhe House of Young Scientists.

REFERENCES

1 Kingsmore, S. F. 2006 Multiplexed protein measurement: technologies and applications of protein and antibody arrays. *Nat. Rev. Drug Discov.* **5**, 310–321. (doi:10.1038/nrd2006)
2 Sahab, Z. J., Semaan, S. M. & Sang, X. A. 2007 Methodology and applications of disease biomarker identification in human serum. *Biomarker Insights* **2**, 21–43.
3 Tahara, H. *et al.* 2009 Emerging concepts in biomarker discovery; the US-Japan workshop on immunological molecular markers in oncology. *J. Transl. Med.* **7**, 45. (doi:10.1186/1479-5876-7-45)
4 Wulfkuhle, J. D., Liotta, L. A. & Petricoin, E. F. 2003 Proteomic applications for the early detection of cancer. *Nat. Rev. Cancer* **3**, 267–275. (doi:10.1038/nrc1043)
5 Berglund, L. *et al.* 2008 A genecentric human protein atlas for expression profiles based on antibodies. *Mol. Cell. Proteomics* **7**, 2019–2027. (doi:10.1074/mcp.R800013-MCP200)
6 Nilsson, P. *et al.* 2005 Towards a human proteome atlas: high-throughput generation of mono-specific antibodies for tissue profiling. *Proteomics* **5**, 4327–4337. (doi:10.1002/pmic.200500072)
7 Ponten, F. *et al.* 2009 A global view of protein expression in human cells, tissues, and organs. *Mol. Syst. Biol.* **5**, 337. (doi:10.1038/msb.2009.93)
8 Uhlen, M. *et al.* 2005 A human protein atlas for normal and cancer tissues based on antibody proteomics. *Mol. Cell. Proteomics* **4**, 1920–1932. (doi:10.1074/mcp.M500279-MCP200)
9 Tessler, L. A., Reifenberger, J. G. & Mitra, R. D. 2009 Protein quantification in complex mixtures by solid phase single-molecule counting. *Anal. Chem.* **81**, 7141–7148. (doi:10.1021/ac901068x)

10 Wingren, C. & Borrebaeck, C. A. 2009 Antibody-based microarrays. *Methods Mol. Biol.* **509**, 57–84. (doi:10.1007/978-1-59745-372-1_5)
11 Aebersold, R. & Mann, M. 2003 Mass spectrometry-based proteomics. *Nature* **422**, 198–207. (doi:10.1038/nature01511)
12 Gstaiger, M. & Aebersold, R. 2009 Applying mass spectrometry-based proteomics to genetics, genomics and network biology. *Nat. Rev. Genet.* **10**, 617–627. (doi:10.1038/nrg2633)
13 Han, X., Aslanian, A. & Yates III, J. R. 2008 Mass spectrometry for proteomics. *Curr. Opin. Chem. Biol.* **12**, 483–490. (doi:10.1016/j.cbpa.2008.07.024)
14 Pan, S., Aebersold, R., Chen, R., Rush, J., Goodlett, D. R., McIntosh, M. W., Zhang, J. & Brentnall, T. A. 2009 Mass spectrometry based targeted protein quantification: methods and applications. *J. Proteome Res.* **8**, 787–797. (doi:10.1021/pr800538n)
15 Carlsson, A., Wingren, C., Ingvarsson, J., Ellmark, P., Baldertorp, B., Ferno, M., Olsson, H. & Borrebaeck, C. A. 2008 Serum proteome profiling of metastatic breast cancer using recombinant antibody microarrays. *Eur. J. Cancer* **44**, 472–480. (doi:10.1016/j.ejca.2007.11.025)
16 Haab, B. B. 2006 Applications of antibody array platforms. *Curr. Opin. Biotechnol.* **17**, 415–421. (doi:10.1016/j.copbio.2006.06.013)
17 Mendoza, L. G., McQuary, P., Mongan, A., Gangadharan, R., Brignac, S. & Eggers, M. 1999 High-throughput microarray-based enzyme-linked immunosorbent assay (ELISA). *Biotechniques* **27**, 778–780.
18 Moody, M. D., Van Arsdell, S. W., Murphy, K. P., Orencole, S. F. & Burns, C. 2001 Array-based ELISAs for high-throughput analysis of human cytokines. *Biotechniques* **31**, 186–190.
19 Ellmark, P., Ghatnekar-Nilsson, S., Meister, A., Heinzelmann, H., Montelius, L., Wingren, C. & Borrebaeck, C. A. 2009 Attovial-based antibody nanoarrays. *Proteomics* **9**, 5406–5413. (doi:10.1002/pmic.200800962)
20 Lausted, C. G., Warren, C. B., Hood, L. E. & Lasky, S. R. 2006 Printing your own inkjet microarrays. *Methods Enzymol.* **410**, 168–189. (doi:10.1016/S0076-6879(06)10008-7)
21 Lee, K. B., Park, S. J., Mirkin, C. A., Smith, J. C. & Mrksich, M. 2002 Protein nanoarrays generated by dip-pen nanolithography. *Science* **295**, 1702–1705. (doi:10.1126/science.1067172)
22 Schena, M., Shalon, D., Davis, R. W. & Brown, P. O. 1995 Quantitative monitoring of gene expression patterns with a complementary DNA microarray. *Science* **270**, 467–470. (doi:10.1126/science.270.5235.467)
23 Diercks, A. H., Ozinsky, A., Hansen, C. L., Spotts, J. M., Rodriguez, D. J. & Aderem, A. 2009 A microfluidic device for multiplexed protein detection in nano-liter volumes. *Anal. Biochem.* **386**, 30–35. (doi:10.1016/j.ab.2008.12.012)
24 Barbee, K. D. & Huang, X. H. 2008 Magnetic assembly of high-density DNA arrays for genomic analyses. *Anal. Chem.* **80**, 2149–2154. (doi:10.1021/ac702192y)
25 Barbee, K. D., Hsiao, A. P., Heller, M. J. & Huang, X. 2009 Electric field directed assembly of high-density microbead arrays. *Lab Chip* **9**, 3268–3274. (doi:10.1039/b912876j)
26 Barbee, K. D., Hsiao, A. P., Roller, E. E. & Huang, X. 2010 Multiplexed protein detection using antibody-conjugated microbead arrays in a microfabricated electrophoretic device. *Lab Chip* **10**, 3084–3093. (doi:10.1039/c0lc00044b)
27 Blicharz, T. M., Siqueira, W. L., Helmerhorst, E. J., Oppenheim, F. G., Wexler, P. J., Little, F. F. & Walt, D. R. 2009 Fiber-optic microsphere-based antibody array for the analysis of inflammatory cytokines in saliva. *Anal. Chem.* **81**, 2106–2114. (doi:10.1021/ac802181j)
28 Szurdoki, F., Michael, K. L. & Walt, D. R. 2001 A duplexed microsphere-based fluorescent immunoassay. *Anal. Biochem.* **291**, 219–228. (doi:10.1006/abio.2001.5041)
29 Fulton, R. J., McDade, R. L., Smith, P. L., Kienker, L. J. & Kettman Jr, J. R. 1997 Advanced multiplexed analysis with the FlowMetrix system. *Clin. Chem.* **43**, 1749–1756.
30 Nolan, J. P. & Mandy, F. 2006 Multiplexed and microparticle-based analyses: quantitative tools for the large-scale analysis of biological systems. *Cytometry A* **69**, 318–325.
31 Schwenk, J. M., Igel, U., Kato, B. S., Nicholson, G., Karpe, F., Uhlen, M. & Nilsson, P. 2009 Comparative protein profiling of serum and plasma using an antibody suspension bead array approach. *Proteomics* **10**, 532–540. (doi:10.1002/pmic.200900657)
32 Birtwell, S. & Morgan, H. 2009 Microparticle encoding technologies for high-throughput multiplexed suspension assays. *Integr. Biol.* **1**, 345–362. (doi:10.1039/B905502A)
33 Ferguson, J. A., Steemers, F. J. & Walt, D. R. 2000 High-density fiber-optic DNA random microsphere array. *Anal. Chem.* **72**, 5618–5624. (doi:10.1021/ac0008284)
34 Fournier-Bidoz, S., Jennings, T. L., Klostranec, J. M., Fung, W., Rhee, A., Li, D. & Chan, W. C. 2008 Facile and rapid one-step mass preparation of quantum-dot barcodes. *Angew. Chem. Int. Ed. Engl.* **47**, 5577–5581. (doi:10.1002/anie.200800409)
35 Han, M., Gao, X., Su, J. Z. & Nie, S. 2001 Quantum-dot-tagged microbeads for multiplexed optical coding of biomolecules. *Nat. Biotechnol.* **19**, 631–635. (doi:10.1038/90228)
36 Michael, K. L., Taylor, L. C., Schultz, S. L. & Walt, D. R. 1998 Randomly ordered addressable high-density optical sensor arrays. *Anal. Chem.* **70**, 1242–1248. (doi:10.1021/ac971343r)
37 Rauf, S., Glidle, A. & Cooper, J. M. 2009 Production of quantum dot barcodes using biological self-assembly. *Adv. Mater.* **21**, 4020–4024. (doi:10.1002/adma.200900223)
38 Wong, J., Sibani, S., Lokko, N. N., LaBaer, J. & Anderson, K. S. 2009 Rapid detection of antibodies in sera using multiplexed self-assembling bead arrays. *J. Immunol. Methods* **350**, 171–182. (doi:10.1016/j.jim.2009.08.013)
39 Fan, R. *et al.* 2008 Integrated barcode chips for rapid, multiplexed analysis of proteins in microliter quantities of blood. *Nat. Biotechnol.* **26**, 1373–1378. (doi:10.1038/nbt.1507)
40 Klostranec, J. M., Xiang, Q., Farcas, G. A., Lee, J. A., Rhee, A., Lafferty, E. I., Perrault, S. D., Kain, K. C. & Chan, W. C. 2007 Convergence of quantum dot barcodes with microfluidics and signal processing for multiplexed high-throughput infectious disease diagnostics. *Nano Lett.* **7**, 2812–2818. (doi:10.1021/nl071415m)
41 Sedgwick, H., Caron, F., Monaghan, P. B., Kolch, W. & Cooper, J. M. 2008 Lab-on-a-chip technologies for proteomic analysis from isolated cells. *J. R. Soc. Interface* **5**, S123–S130. (doi:10.1098/rsif.2008.0169.focus)
42 Abramoff, M. D., Magelhaes, P. J. & Ram, S. J. 2004 Image processing with ImageJ. *Biophotonics Intl* **11**, 36–42.
43 Otsu, N. 1979 A threshold selection method from gray-level histograms. *IEEE Trans. Syst. Man Cybern.* **9**, 62–66. (doi:10.1109/TSMC.1979.4310076)
44 Findlay, J. & Dillard, R. 2007 Appropriate calibration curve fitting in ligand binding assays. *AAPS J.* **9**, E260–E267. (doi:10.1208/aapsj0902029)
45 Kung, L. A. & Snyder, M. 2006 Proteome chips for whole-organism assays. *Nat. Rev. Mol. Cell Biol.* **7**, 617–622. (doi:10.1038/nrm1941)
46 Chao, T. C. & Ros, A. 2008 Microfluidic single-cell analysis of intracellular compounds. *J. R. Soc. Interface* **5**(Suppl. 2), S139–S150. (doi:10.1098/rsif.2008.0233.focus)